



Automatically Generating Websites from Hand-drawn Mockups

João Silva Ferreira¹, André Restivo² and Hugo Sereno Ferreira³

¹Faculdade de Engenharia da Universidade do Porto, Portugal

²Faculdade de Engenharia da Universidade do Porto, LIACC, Portugal

³Faculdade de Engenharia da Universidade do Porto, INESC TEC, Portugal

Keywords: Synthetic Datasets, Neural Networks, Computer Vision, Real-time, Website Generation.

Abstract: Designers often use physical hand-drawn mockups to convey their ideas to stakeholders. Unfortunately, these sketches do not depict the exact final look and feel of web pages, and communication errors will often occur, resulting in prototypes that do not reflect the stakeholder's vision. Multiple suggestions exist to tackle this problem, mainly in the translation of visual mockups to prototypes. Some authors propose end-to-end solutions by directly generating the final code from a single (black-box) Deep Neural Network. Others propose the use of object detectors, providing more control over the acquired elements but missing out on the mockup's layout. Our approach provides a real-time solution that explores: (1) how to achieve a large variety of sketches that would look indistinguishable from something a human would draw, (2) a pipeline that clearly separates the different responsibilities of extracting and constructing the hierarchical structure of a web mockup, (3) a methodology to segment and extract containers from mockups, (4) the usage of in-sketch annotations to provide more flexibility and control over the generated artifacts, and (5) an assessment of the synthetic dataset impact in the ability to recognize diagrams actually drawn by humans. We start by presenting an algorithm that is capable of generating synthetic mockups. We trained our model (N=8400, Epochs=400) and subsequently fine-tuned it (N=74, Epochs=100) using real human-made diagrams. We accomplished a mAP of 95.37%, with 90% of the tests taking less than 430ms on modest commodity hardware (≈ 2.3 fps). We further provide an ablation study with well-known object detectors to evaluate the synthetic dataset in isolation, showing that the generator achieves a mAP score of 95%, $\approx 1.5 \times$ higher than training using hand-drawn mockups alone.


1 INTRODUCTION


When designing a web page, professionals usually resort to rough sketches to communicate and discuss their ideas (Weichbroth and Sikorski, 2015). The very nature of these mockups (*i.e.* basically lines) transmits the idea of the elements, that will occupy certain parts of the layout, by the usage of agreed symbols. The particular symbols may vary from culture to culture and are generally the target study of *semiotics* (Eco et al., 1976). But as long as the collaborating parties agree to use the same symbols, mockups become an efficient way to convey the general ideas behind a work without its (time-consuming) specificities. A prototype is then subsequently implemented, and the iteration restarts.

In this proposal, we aim to shorten the *feedback loop* cycle to achieve *real-time* HTML generation

from hand-drawn sketches, while ensuring overall accuracy (Aguar et al., 2019). With the rise and reliability of neural networks, the interpretation of mockups became feasible by resorting to *object detectors* (Redmon et al., 2017; Ren et al., 2017; Suleri et al., 2019), or by generating text descriptions from an image (You et al., 2016; Karpathy and Fei-Fei, 2015).

To train these models, a varied and large number of examples is necessary. But in many cases, this data is (a) non-existent, (b) missing required annotations, (c) low-quality, with errors or untrustable, or (d) not generally appropriate for the specific needs of a project. This leaves only one straightforward, though arguably easy, solution: to draw the dataset by hand (Ellis et al., 2018; Yun et al., 2019a). To circumvent this problem, we will also present a mechanism that automatically generates a large set of digital hand-drawn-like mockups.

^a <https://orcid.org/0000-0002-1328-3391>

^b <https://orcid.org/0000-0002-4963-3525>

2 RELATED WORK

One of the earliest attempts of interpreting human-made sketches was proposed by Landay *et al.* (Landay, 1995), which used a digital input device (such as a stylus or a mouse) to classify and transform designer drawings into their respective elements. But complete translations of hand-drawn web pages to an (almost final) prototype is something that gained increased interest in the last years. We now provide a summary of current related work and categorize their strategies.

2.1 Heuristic based Methodologies

These methodologies make usage of “classic” computer vision algorithms, such as thresholding and morphological operations, where a sequence of procedures is executed iteratively until the elements that compose the mockup are extracted. Hassan *et al.* (Hassan *et al.*, 2018) explore object hierarchy using a top-down approach, where the atomic elements are first gathered and removed from the main image, and then containers are detected. A bottom-up approach is done by Huang *et al.* (Huang *et al.*, 2016), others add the ability to detect and recognize text (Nguyen and Csallner, 2015)(Kim *et al.*, 2018b).

2.2 End-to-End Methodologies

Recent advances in Deep Neural Networks (DNNs) made holistic approaches regarding the training and responsibility of the final network possible. Pix2code (Beltramelli, 2018) seems to be one of the earliest works and served as inspiration for other authors (Chen *et al.*, 2018). They divide their approach into three subproblems: (1) scene understanding, by inferring the properties of the elements in an image, (2) language modeling, in order to generate syntactically and semantically correct code, and (3) final aggregation, relating detected objects with their respective code. The solution is a model composed of Convolutional Neural Networks (CNNs) and Long-Short Term Memory (LSTMs), which convert images to intermediate representations. The work done by Zhihao *et al.* (Zhu *et al.*, 2018) improves previous works by removing the need to feed the network with initial context, thus creating a complete end-to-end model.

2.3 Object Detection Methodologies

Object detectors focus on extracting the bounding boxes of elements in a given image. Suleri *et al.* (Suleri *et al.*, 2019) describe a sketch-based prototyp-

ing workbench that works in three levels of fidelities: low, medium, and high. The user can interact with each particular level by (1) tweaking the mockup or its interactions, (2) monitoring the conversion process from drawings to detection, possibly labeling undetected elements, and (3) applying themes and generating the target code. Yun *et al.* (Yun *et al.*, 2019b) make use of the popular YOLO (Redmon *et al.*, 2017) detection system to recognize the elements presented in a mockup, by resorting to a custom annotation language that improves the identification of the element’s type. Kim *et al.* (Kim *et al.*, 2018a) use Faster R-CNN (Redmon *et al.*, 2017) to detect the elements, and add a step for layout detection by resorting to a slope filtering technique that avoids non-horizontal/vertical lines.

2.4 Data Driven Methodologies

Moran *et al.* (Moran *et al.*, 2018) explore the usage of hierarchy already present in known UIs, based on the premise that the designer intends to create something that already exists. Their strategy is divided into 3 phases: detection, classification, and assembly. Detection uses traditional computer vision techniques to extract the location of the elements. Classification relies on elements’ locations to classify them by using a previously-trained CNN on a real-world examples dataset. The assembly phase uses a KNN algorithm to compare the current elements to existing apps to map the detected elements to real-world examples.

2.5 Synthetic Generators

Previous work in generating synthetic mockups includes the already mentioned Suleri *et al.* (Suleri *et al.*, 2019). To train their model, they crafted a synthetic dataset from real hand-drawings by collecting hand-drawn sketches of different elements, and subsequently sampling the collected UI elements and randomly positioning them to form the final layout.

Other authors working in different domains are attempting to solve the same fundamental problems. Masi *et al.* (Masi *et al.*, 2016) question the necessity of acquiring faces for effective face recognition, with their work modifying an existing dataset to supplement it with facial variations; their results show that such synthesis leads to an increase in recognition accuracy. Kar *et al.* (Kar *et al.*, 2019) propose a 3D engine capable of rendering the scene and additional masks without the need for extra steps. They developed a DNN capable of procedural generation of scenes, by first analyzing real images to learn how to generate synthetic scenes with similar distributions.

The presented methodology evidences content generation improvements when comparing to the respective baseline. And Bernardino *et al.* (Bernardino et al., 2018) show how the generation of a synthetic image dataset based on a 3D human-body model simulating knee injury recovering patients can be used to improve the performance of DNNs designed for goniometry. The model's robustness to noise and varied backgrounds, typical of mobile-phone pictures taken in rehabilitation clinics, is of particular interest.

3 FROM MOCKUPS TO CODE

Our approach consists of a four-step pipeline that receives an image as input and outputs the generated website in *real-time*. The four steps are the following: (1) image acquisition and pre-processing, (2) object and container detection, (3) building the object hierarchy, and (4) HTML-code generation, using a CSS-grid, which better suits our hierarchy approach when compared to the usual linear layouts. Figure 1 contains a summary of this process.

3.1 Image Acquisition

Acquiring real-world images is subject to internal and external factors. Internal factors include those such as the quality of the sensor used by the camera and the lenses used. External factors are the weather, amount, and quality of light and surface texture and reflection. The main goal of this step is to filter such anomalies and convert the original image to a high contrast version. The reason behind this approach is directly connected to the detection phase, where DNNs are trained using high contrast images. A popular alternative is to resort to data augmentation techniques during learning that synthetically emulate real-world artifacts.

Here, we first convert the image to black and white and then apply an adaptive threshold to define the lines of the mockup where the illumination is irregular better. This results in a high contrast image, which can still have some noise. We proceed with two morphological operations using a structuring element in the shape of an ellipse: *closing* and *erosion*. The adaptive threshold and structuring element parameters are fully configurable in run-time to fine-tune the final result. Figure 2 illustrates these steps.

3.2 Element Detection

This two-module phase is responsible for the detection of the different elements presented on the sketch, each one expecting to receive an image and return

the detected elements: (a) a module responsible for the detection of each atomic element, and (b) a module responsible for the extraction of containers, where containers are defined by a box including atomic elements such as buttons or text elements. Examples of atomic elements can be found in Figure 3.

For the detection of elements, we used YOLO, by training it with two different datasets: First, we used a mockup generator tool which only generates high contrast mockups with their respective labels (N=8400, Epochs=400). Then, we fine-tuned it using real hand-drawn images (N=107, Epochs=100). The final output of this module is a list of the elements detected, including their class and bounding boxes.

For the extraction of the containers, Pix2Pix and YOLO were used together to extract their bounding box information better. Pix2Pix is based on conditional adversarial networks and provides a general-purpose solution to output an image when given an image as input. We used its ability and trained it to generate figures with just containers. Then, we fed the resulting image to YOLO so it could extract the bounding boxes. Both models were trained using the same amount of data and epochs of the previous module, as well as applying the same fine-tuning process. The training loss values for the element and container detection models can be consulted as supplementary material. The output of both modules was concatenated, resulting in a container and element list, and their classes and bounding boxes.

3.3 Element Pre-processing

The previous steps have produced a single flat list without any hierarchy. We now execute several modules in sequence to extract hierarchical information, with the first operation being the merge between elements and containers. This merge is done linearly, where the intersection of each element is tested against containers, and if more than a certain threshold is met, it is considered inside it. We proceed through each container and assign them with annotation meta-data. These annotations are small symbols that can be used to rapidly modify properties of the containers, providing richer interactions using the same drawing as a base.

Checkboxes and radio buttons are also commonly placed next to lines of text, so we now compare the horizontal collisions with nearby text-blocks. Each checkbox uses its bounding box and expands it horizontally. If a textbox is detected, then a small horizontal container is created with the type of the main element (in this case, checkbox), and both elements are aggregated. This step continues until all check-

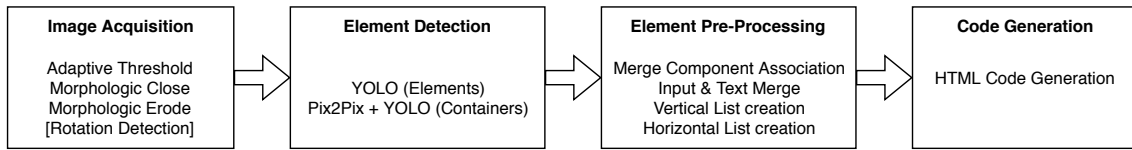


Figure 1: Pipeline processing steps executed sequentially.

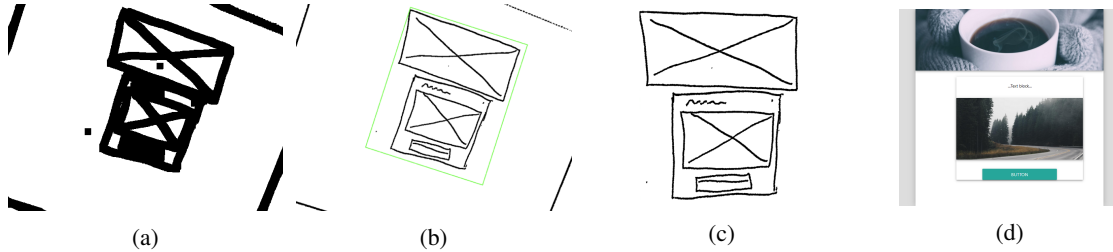


Figure 2: Image Acquisition Process and Final Result executed in sequential order: (a) The resulting image from the adaptive threshold and morphological operations, (b) Small area rectangle detection, (c) Mockup cropped and rotation corrected, and after several steps, (d) Generated website.

boxes/radio buttons are processed.

Web pages also tend to organize their contents in lists, so sequences of elements of the same kind are list-aggregated. First, all elements are evaluated against their type by expanding their bounding boxes vertically. If the box intersects with another object of the same type, it is selected as a candidate for the list. We proceed to check if anything is in between the current object (used to search for similar objects) and the newly acquired object. If nothing is, then the element is stored, and all the collected elements are stored in a horizontal container with the type of the inserted elements. The same procedure is then applied horizontally.

The final step is the aggregation of all elements to generate a more concise hierarchy. We propose a Hierarchy Reconstruction Algorithm, which main idea is that, at any point, a container may be subdivided into horizontal or vertical layouts. The algorithm starts with the root container, which has all the elements and subgroups up until this point. Then, we attempt to separate the elements in a given orientation (horizontal or vertical). When testing a given orientation, the elements are sorted accordingly.

For example, consider the layout depicted in Figure 5; let's assume the expanding orientation is vertical. After the elements are sorted vertically, the first one is selected as a starting point; then, a *testing box* is created to identify elements that relate to the starting object. The *testing box* has the dimensions of the container's and the object's bounds (Figure 5b). Since the expansion is vertical, the box that is created has a horizontal dimension equal to the container's boundaries, and a vertical dimension equals to the selected object. With the *testing box* in place, the remaining children

of the container are tested; in the case where they fit this box, it is updated to accommodate the newly inserted elements. This behavior repeats until an object fails to overlap with the box (Figure 5c). Should this happen, the result is added to a list. In case the number of elements inside of the box is one, then only the item is added; otherwise, a new container is created and all the elements inside of the box are added to this container as children. The algorithm then repeats until all the container's elements are added to their own list (Figure 5d). The result of this algorithm is always a list of elements.

Should the resulting list contain only one object, it is considered not to be possible to separate the elements in that given direction, and thus the alternative is tested. In the case where elements cannot be separated in any direction, then this container is marked as a grid, and the execution continues. This algorithm is then applied to each container child with the opposite orientation (Figure 5e).

The result is a hierarchy where the elements are associated with their respective containers and are organized as horizontal and vertical lists.

3.4 Code Generation

With the final hierarchy, all is ready to feed into the HTML/CSS generators. Our generator uses containers and their previously attached attributes to apply custom CSS tags, thus changing the style of said element. To generate the HTML, the hierarchy is iterated in a *depth-first* fashion, with each element being translated to a corresponding HTML component. For containers that are not represented as lists, they are marked as a CSS-grid. Their children use the rela-

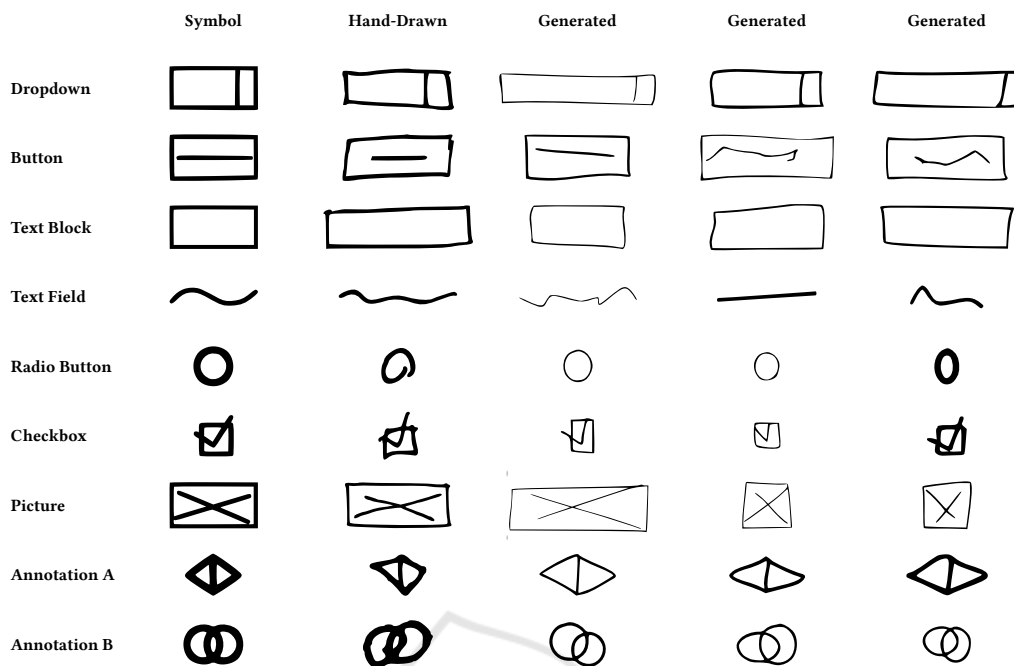


Figure 3: Left-to-right, examples of (1) atomic elements, (2) hand-drawn elements, and (3) (4) (5) generated specimens used in our work. The morphological variety of the synthetic elements is produced by us, using an algorithm soon to be published.

tive position and size to define the location inside the grid. The default value of grid cells in the horizontal space is arbitrarily defined as 8; the vertical space is calculated by comparing the width of the cell and using this value for calculating the number of cells in the vertical axis. Containers that are tagged as horizontal or vertical lists do not need this snapping step and thus are generated sequentially. The final result is displayed in *real-time* in a browser window. Figure 7 provides examples of the result.

3.5 Synthetic Mockups

Most steps in this pipeline are based on machine learning models, which, to be trained, need a varied and large number of examples. Drawing them by hand was too time consuming and not a viable option; so a process to automatically generate an extensive set of hand-drawn-like mockups was needed. Our solution is described in the next few sections.

We can think of webpages as being composed of two kinds of elements: (1) the *atomic elements*, such as buttons, text fields, and radio buttons, and (2) *containers*, which encapsulate said components into semantically and structurally meaningful groups. Our solution takes both concepts into account. Although we present results for a single layer of containers, this procedure can be recursively applied to allow containers inside other containers. Our process for mockup

generation is sequential and organized in the following steps, depicted in Figure 6.

3.5.1 Boundaries Calculation

Let there be a canvas of *width* and *height*. To select the mockup bounding box, we draw the *cell size* and *cell gap* values from a random bounds distribution. The canvas is subsequently divided, horizontally and vertically, by the *grid size* and *gap*. The remaining space is regarded as *margins*, used for placement offset equally chosen at random (Figure 6b). This step enables the division of the mockup into several cells where we can later place components.

3.5.2 Container Placement

As containers are used to semantically and structurally group different elements together, their area is assumed to be higher than a single cell. Previously calculated cells are used to displace the containers over the grid, incidentally simplifying the later placement of atomic elements. We then go through it from *top-left* to *bottom-right*. For each unoccupied cell, random values are drawn for the horizontal and vertical expansion values of the element (i.e., number of cells), taking into account the remaining space available to preserve established boundaries. The next step checks the neighboring areas for overlapping containers (cells already in use). For each cell visited, the

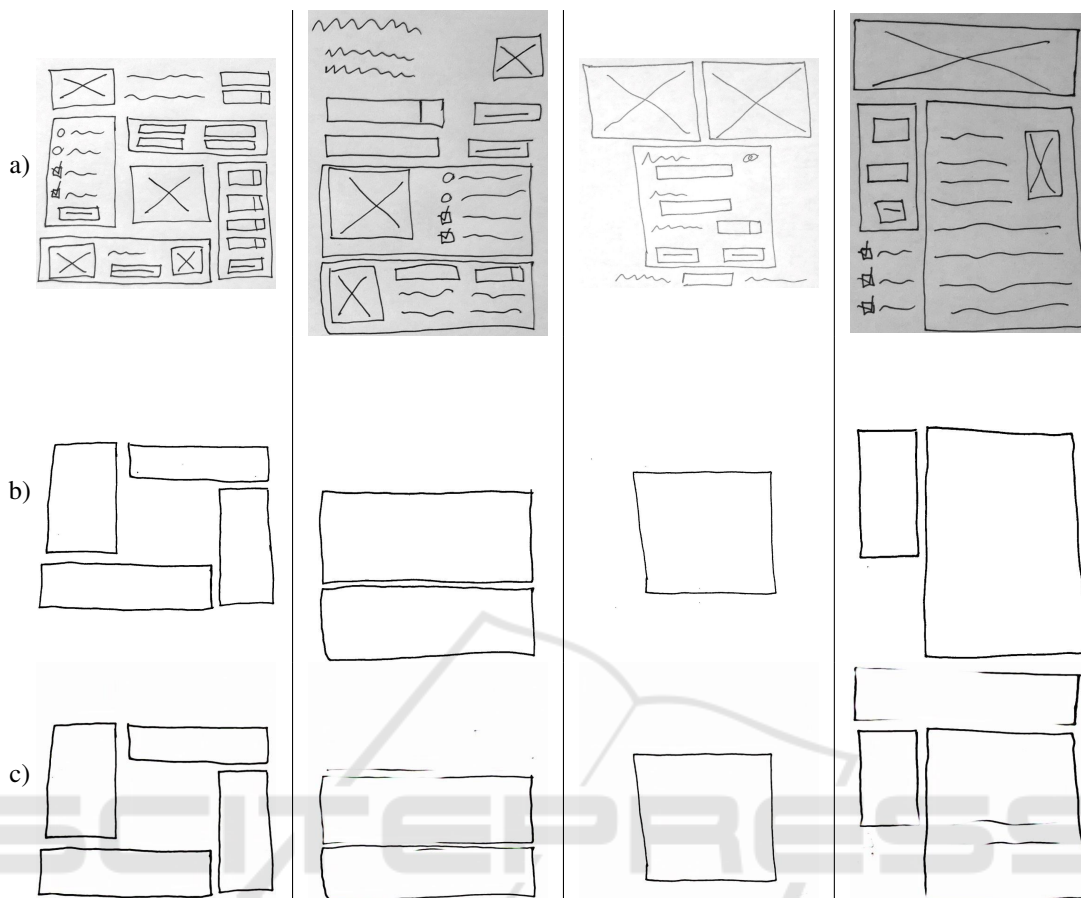


Figure 4: Four examples of container segmentation/extracted by Pix2pix: (a) the input image, (b) the ground truth, and (c) the output result.

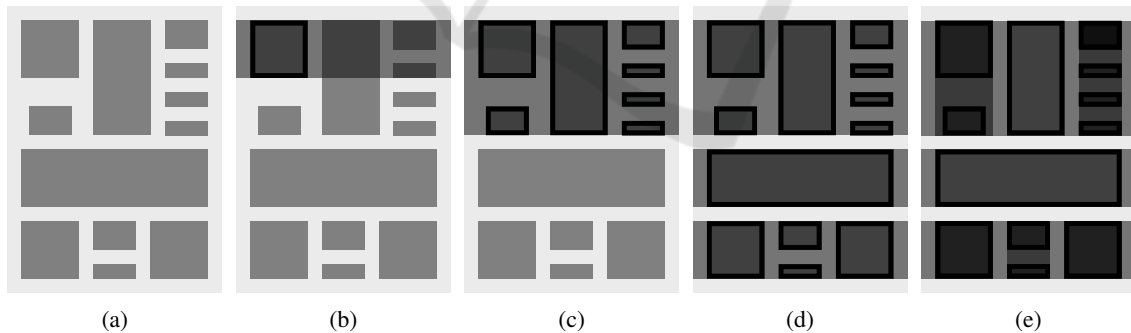


Figure 5: Hierarchy Generation Algorithm: (a) Original hierarchy, (b) First element selected and Testing Box expanded horizontally, (c) Testing Box expanded to Accommodate all elements, (d) Process repeated for the remaining elements, and (e) Process applied to the generated sub-containers vertically.

boundary is updated; in case neighbors are detected, the container stops its expansion, and the previous boundary is used. Finally, the candidate boundary is evaluated and discarded if it does not meet the requirements (here, an area greater than two). At the end of this process, the containers are considered defined and ready to be filled with elements. Figure 6c depicts the results so far.

3.5.3 Element Area Definition

The procedure to fill the cells with the elements follows a process similar to that of the containers. The only difference is that the container's area is taken into account.

At the end of the previous step, all cells are associated with the container they belong to by tagging

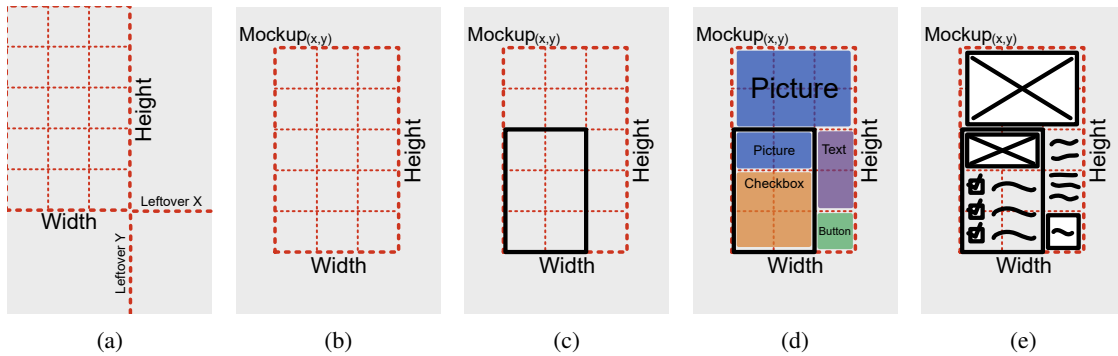


Figure 6: High-level overview of our approach, executed in a sequential order: (a) Mockup dimension and leftover calculation, (b) Mockup translation, (c) Container placement, (d) Element area definition, and (e) Element placement.

them with an ID. In this step we apply the same rationale to generate new random values and expand elements horizontally or vertically. For each cell inside the bounds, a check is made to collect cells that match the container ID and are empty. In case of a possible collision, which can occur if (1) a cell belongs to a different container, or (2) a cell is already occupied, the algorithm stops and uses the previous available coordinates as the bound limit. This enables the definition of multiple areas representing different kinds of elements, which will be later expanded to fill their respective bounds. The result of this phase is represented in Figure 6d.

3.5.4 Element Placement

As the grid is already populated with containers and areas representing the kind of element which must be placed into, this step is responsible for filling said areas, depending on multiple parameters that were defined to determine the filling behavior of each area. For elements such as images, only one element is added to that area with the same size as the specified bounds. With small and/or grouped elements such as checkboxes, it makes sense to limit its shape size to a semantically natural one. So instead of filling the whole area with a giant checkbox, we use it to place multiple checkboxes representing them as vertical lists.

Defining the placement of these lists is similar to the way the mockup boundaries are calculated. Each element has a random target height that falls within a pre-specified bound. Given the list item height, the full area height is used to calculate the number of elements that the list could fit and the remaining margin. Once this margin is calculated, the whole list is displaced by a random factor of said margin, and the items are created. In the case of buttons, this operation is straightforward. But in the case of checkboxes or radio buttons, since each of these items usually has

Table 1: Element’s fill parameters. The expansion column represents if the element will expand vertically, horizontally or both. The split value indicates if expansion would be done by enlarging or creating new elements (in the given direction). The height contains the intervals used to define the element’s size. Finally, we also provide an option to fill the remaining horizontal space with text.

Element	Expansion	Split	Height	Text
Picture	both	none	none	
Radio Button	vertical	vertical	[40;50]	•
Checkbox	vertical	vertical	[40;50]	•
Dropdown	horizontal	vertical	[40;70]	
Text field	horizontal	vertical	[40;70]	
Text block	both	vertical	[40;70]	
Button	both	vertical	[40;70]	

the aspect ratio of 1:1, a highly unoccupied horizontal space can exist. To enrich these elements another parameter is considered that lets the generator place text over the unused horizontal space. This creates a more natural way of defining lists, where each checkbox is placed near a text description. Table 1 contains the rules used to fill the area of a given element. Figure 6e represents the results of element expansion, namely in the areas belonging to texts and checkboxes.

3.5.5 Elements Drawing Process

Once in this phase, the grid is filled with different elements, which contain the bounding boxes that define their areas. Would the elements be drawn as currently set, the result would be perfectly straight lines which are not expected from hand-drawn mockups. To add more variety and make them closer to what a human would sketch, we make further adjustments to the geometry that dictates the final shape of each element.

We currently apply two types of adjustments. First, we offset each vertices comprising the element shape by a random value, which creates the possibility of non-parallel lines. As a side effect of this op-

eration, there's a probability that the element might look slightly rotated. Then, we target the unintended uniformity when drawing an edge. We preserve the original ends while adding multiple points positioned randomly along the line, thus creating distortions in the final drawing. We further make usage of bowing, roughness, brush size, and other drawing strategies that simulate the distinct styles of different drawing instruments such as sharpies, pens, or pencils.

Figure 3 provides several examples of this step when applied to different elements, such as buttons, text fields, and checkboxes, and compares them to hand-drawn sketches.

4 EVALUATION

To assess our approach, we prioritized the evaluation of the detection phase by measuring the mean average precision (mAP) and the log-average miss rate (LAMR), as both elements are useful to evaluate the overall performance in the object detection task (Ren et al., 2017; Redmon et al., 2016; Girshick et al., 2014; Suleri et al., 2019; Razavian et al., 2014; Wojek et al., 2011; Zhao et al., 2018). The mean average precision plots the precision and recall curves for each class and then proceeds to calculate a simplified area. The mean of every area calculated is then taken into account to compute the final mAP score. The LAMR is defined by averaging the miss rates, where *miss rate* is defined as $MR = FN / (TP + FN)$ as proposed by Wojek *et al.* (Wojek et al., 2011) to evaluate and compare the performance stably.

The detection phase is comprised of the element and container detection steps. The container detection phase, as mentioned before, is composed of two models executed in sequence, starting with Pix2Pix and ending with YOLO. This phase was evaluated as a whole, thus reflecting the interactions and final results from these models. The results of mAP and LAMR can be consulted in Table 2. As the *real-time* constraint is paramount to our work, the execution time of the whole system was also evaluated in very modest commodity hardware (see Table 3).

5 RESULTS AND DISCUSSION

The detection performance of our approach achieved a mAP score of 95.37%, which shows **overall good element detection**. The LAMR of some components, such as checkboxes and annotation elements, still needs further work. We have also observed that **the container phase is the most critical** to obtain

good (hierarchically sound) results. Future improvements of this system should focus on reducing the false positives, which could easily be attenuated with longer training and a larger dataset. Earlier during our research, we experimented with U-NET to isolate containers, but the network could not generalize well, probably due to the thin size of the container lines. The usage of Pix2Pix model improved the results substantially, but at the cost of execution performance. In fact, **the container detection phase has the highest impact in execution time**, accounting for 98% of the total work on average. However, in 90% of the cases we tested (N=107), the process was executed entirely (from image acquisition to HTML generation) in less than 414ms using our hardware. It should be noted that **the final system is sensitive to camera perspective**, which can result in wrongly-rotated images and misaligned boundaries. This can be solved either by resorting to added modules during pre-processing, or data-augmentation techniques during learning. Fortunately, our *real-time* approach allows the designer to correct these cases quickly. There is enough evidence that our approach improves the result of object detection using current state-of-the-art techniques (here YOLO), by augmenting a hand-drawn dataset using synthetically generated mockups.

The results from boosting our system with synthetic datasets are also considerably better when compared to the baseline, highlighting an overall better mAP (95.3%) and log-average miss rate in every element evaluated. The false positives are also significantly lower when compared to the other two models, and there's also an increase in the true positives. We show that the **difference in performance cannot be attributed to the sheer size of the training data**, as the mAP of these models is extremely close (59.7% vs 60.5%).

6 CONCLUSIONS

Designers often use physical hand-drawn mockups to convey their ideas to stakeholders. In this paper, we proposed a multi-stage pipelined solution mixing heuristics and machine learning approaches to produce a *real-time* system that generates HTML/CSS from human-made sketches.

Our solution has the object detection phase at the heart of the pipeline. Even though some errors/misses might occur in the detection phase, the detected elements can still be placed according to the detected location, something that pure end-to-end models struggle with, and usually produce strange hierarchies. Our pipeline architecture also has the advantage of identi-

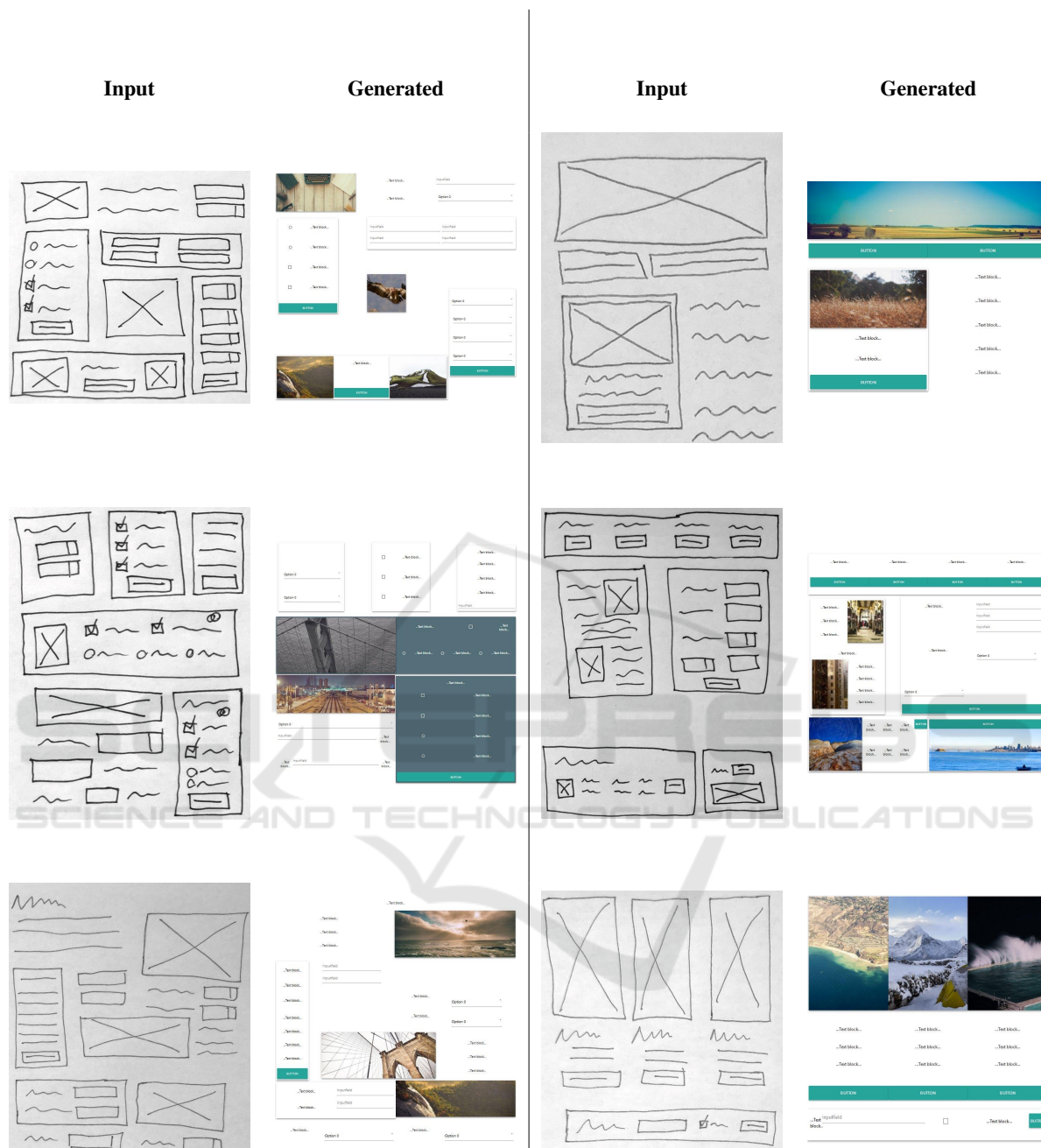


Figure 7: Example of results produced from our approach. The left column contains the captured image without any pre-processing, and using a mobile-phone camera. The right column presents the generated HTML rendered using the Chrome browser.

fyng and checking the progress of the inferred hierarchy, while allowing new strategies to be plugged in. The possible downside is that different models need to be trained individually, which can lead to longer training times and may be difficult to tweak if models are dependent on each other. We, however, are prioritizing *real-time* performance.

The use of a CSS-grid greatly simplifies the hierarchy generations, making possible layouts tricky to produce using linear structures. The detection of lists and aggregation of checkboxes/radio buttons to text blocks also improved the final alignment of the generated web pages. This phase still has plenty of room for exploration, particularly in the definition of

Table 2: Detection Results. From left-to-right, we have training using only hand-drawn examples, only synthetic examples, and with our final approach. For each one, Ground-truth represents the absolute number of elements that exist on the validation dataset. False positives indicate the number of miss detections wrongly classified as the target class. True positives are the correct classifications where a match is present in the dataset. The overall mAP score is 94.6%.

Class	Hand-Drawn				Synthetic				Final				GT
	FP	TP	AP (%)	LAMR	FP	TP	AP (%)	LAMR	FP	TP	AP (%)	LAMR	
TextBlock	24	308	86	0.48	42	231	61	0.78	3	334	97	0.06	345
Picture	6	88	86	0.20	2	84	82	0.19	0	99	97	0.03	102
Button	10	80	83	0.34	76	88	61	0.83	2	92	98	0.05	93
Textfield	21	57	69	0.57	0	15	21	0.79	1	70	97	0.03	72
Checkbox	8	36	43	0.78	12	58	68	0.63	3	64	88	0.20	72
Dropdown	13	42	65	0.49	0	28	47	0.53	2	58	97	0.04	60
RadioButton	6	37	66	0.50	0	42	78	0.22	0	53	98	0.02	54
Component	6	4	86	0.20	0	2	22	0.78	1	8	86	0.20	9

Table 3: Execution times (in milliseconds) of 107 runs on a NVidia GTX 970 and i7 3770k@4.1GHz, using Tensorflow 1.8.0. We provide the mean and the 90th percentile.

Phase	Mean (ms)	90 th P (ms)
Detection (Elements)	120	90
Detection (Containers)	310	276
Detection (Total)	430	275
Processing	3	1
Generation	4	5
Total	438	414

the final hierarchy. Inferring the intended web site hierarchy may be akin to understand its *semantics*, and as such, is a difficult problem. Using models trained with real-world hierarchical information may improve this step.

We also describe an algorithmic approach to the generation of arbitrarily large datasets of labeled synthetic mockups that are able to mimic hand-drawn sketches. This was motivated by the necessity training Deep Neural Networks that can generalize well, thus providing them with good candidates that have exact, high-quality annotations. The particular improvement of this step is independently evaluated, achieving a mAP score $\approx 1.5\times$ higher than training using only hand-drawn mockups.

Overall, our approach achieves good results, with the highest mAP score of 94.6% taking just 414ms from end-to-end generation, translating to ≈ 2 frames-per-second using a modest 2014-era graphics card.

REFERENCES

- Aguiar, A., Restivo, A., Correia, F. F., Ferreira, H. S., and Dias, J. P. (2019). Live software development — tightening the feedback loops. In *Proceedings of the 5th Programming Experience (PX) Workshop*.
- Beltramelli, T. (2018). Pix2Code: Generating Code from a Graphical User Interface Screenshot. In *Proceedings of the ACM SIGCHI Symposium on Engineering Interactive Computing Systems, EICS '18*, pages 3:1—3:6, New York, NY, USA. ACM.
- Bernardino, J., Teixeira, L. F., and Ferreira, H. S. (2018). Bio-measurements estimation and support in knee recovery through machine learning. *CoRR*, abs/1807.07521.
- Chen, C., Su, T., Meng, G., Xing, Z., and Liu, Y. (2018). From UI Design Image to GUI Skeleton: A Neural Machine Translator to Bootstrap Mobile GUI Implementation. In *Proceedings of the 40th International Conference on Software Engineering, ICSE '18*, pages 665–676, New York, NY, USA. ACM.
- Eco, U. et al. (1976). *A theory of semiotics*, volume 217. Indiana University Press.
- Ellis, K., Ritchie, D., Solar-Lezama, A., and Tenenbaum, J. (2018). Learning to infer graphics programs from hand-drawn images. In Bengio, S., Wallach, H., Larochelle, H., Grauman, K., Cesa-Bianchi, N., and Garnett, R., editors, *Advances in Neural Information Processing Systems 31*, pages 6059–6068. Curran Associates, Inc.
- Girshick, R. B., Donahue, J., Darrell, T., and Malik, J. (2014). Rich Feature Hierarchies for Accurate Object Detection and Semantic Segmentation. *2014 IEEE Conference on Computer Vision and Pattern Recognition*, pages 580–587.
- Hassan, S., Arya, M., Bhardwaj, U., and Kole, S. (2018). Extraction and Classification of User Interface Components from an Image. *International Journal of Pure and Applied Mathematics*, 118(24):1–16.
- Huang, R., Long, Y., and Chen, X. (2016). Automatically generating web page from a mockup. *Proceedings of the International Conference on Software Engineering and Knowledge Engineering, SEKE*, 2016-Janua.
- Kar, A., Prakash, A., Liu, M.-Y., Cameracci, E., Yuan, J., Rusiniak, M., Acuna, D., Torralba, A., and Fidler, S.

- (2019). Meta-Sim: Learning to Generate Synthetic Datasets.
- Karpathy, A. and Fei-Fei, L. (2015). Deep visual-semantic alignments for generating image descriptions. In *2015 IEEE Conference on Computer Vision and Pattern Recognition (CVPR)*, pages 3128–3137. IEEE.
- Kim, B., Park, S., Won, T., Heo, J., and Kim, B. (2018a). Deep-learning based web UI automatic programming. In *Proceedings of the 2018 Conference on Research in Adaptive and Convergent Systems - RACS '18*, pages 64–65, New York, New York, USA. ACM Press.
- Kim, S., Park, J., Jung, J., Eun, S., Yun, Y.-S., So, S., Kim, B., Min, H., and Heo, J. (2018b). Identifying UI widgets of mobile applications from sketch images. *Journal of Engineering and Applied Sciences*, 13(6):1561–1566.
- Landay, J. a. (1995). Interactive sketching for user interface design. *Conference companion on Human factors in computing systems - CHI '95*, pages 63–64.
- Masi, I., Tran, A. T., Leksut, J. T., Hassner, T., and Medioni, G. (2016). Do We Really Need to Collect Millions of Faces for Effective Face Recognition?
- Moran, K. P., Bernal-Cardenas, C., Curcio, M., Bonett, R., and Poshyvanik, D. (2018). Machine Learning-Based Prototyping of Graphical User Interfaces for Mobile Apps. *IEEE Transactions on Software Engineering*, 5589(May):1–26.
- Nguyen, T. A. and Csallner, C. (2015). Reverse Engineering Mobile Application User Interfaces with REMAUI (T). In *2015 30th IEEE/ACM International Conference on Automated Software Engineering (ASE)*, pages 248–259.
- Razavian, A. S., Azizpour, H., Sullivan, J., and Carlsson, S. (2014). CNN Features Off-the-Shelf: An Astounding Baseline for Recognition. In *2014 IEEE Conference on Computer Vision and Pattern Recognition Workshops*, pages 512–519. IEEE.
- Redmon, J., Divvala, S., Girshick, R., and Farhadi, A. (2016). You Only Look Once: Unified, Real-Time Object Detection. In *2016 IEEE Conference on Computer Vision and Pattern Recognition (CVPR)*, pages 779–788. IEEE.
- Redmon, J. U. o. W., Divvala, S. A. I. f. A. I., Girshick, R. F. A. R., and Farhadi, A. U. o. W. (2017). You Only Look Once: Unified, Real-Time Object Detection. *Annals of Emergency Medicine*, 70(4):S40.
- Ren, S., He, K., Girshick, R., and Sun, J. (2017). Faster R-CNN: Towards Real-Time Object Detection with Region Proposal Networks. *IEEE Transactions on Pattern Analysis and Machine Intelligence*, 39(6):1137–1149.
- Suleri, S., Sermuga Pandian, V. P., Shishkovets, S., and Jarke, M. (2019). Eve. In *Extended Abstracts of the 2019 CHI Conference on Human Factors in Computing Systems - CHI EA '19*, pages 1–6, New York, New York, USA. ACM Press.
- Weichbroth, P. and Sikorski, M. (2015). User Interface Prototyping. Techniques, Methods and Tools. *Studia Ekonomiczne. Zeszyty Naukowe Uniwersytetu Ekonomicznego w Katowicach*, 234:184–198.
- Wojek, C., Schiele, B., Perona, P., and Doll, P. (2011). Pedestrian Detection : An Evaluation of the State of the Art.
- You, Q., Jin, H., Wang, Z., Fang, C., and Luo, J. (2016). Image Captioning with Semantic Attention. In *2016 IEEE Conference on Computer Vision and Pattern Recognition (CVPR)*, pages 4651–4659. IEEE.
- Yun, Y.-S., Jung, J., Eun, S., So, S.-S., and Heo, J. (2019a). Detection of gui elements on sketch images using object detector based on deep neural networks. In Hwang, S. O., Tan, S. Y., and Bien, F., editors, *Proceedings of the Sixth International Conference on Green and Human Information Technology*, pages 86–90, Singapore. Springer Singapore.
- Yun, Y.-S., Jung, J., Eun, S., So, S.-S., and Heo, J. (2019b). Detection of GUI Elements on Sketch Images Using Object Detector Based on Deep Neural Networks. In Hwang, S. O., Tan, S. Y., and Bien, F., editors, *Proceedings of the Sixth International Conference on Green and Human Information Technology*, pages 86–90, Singapore. Springer Singapore.
- Zhao, Z.-Q., Zheng, P., Xu, S.-t., and Wu, X. (2018). Object Detection with Deep Learning: A Review. *CoRR*, abs/1807.0.
- Zhu, Z., Xue, Z., and Yuan, Z. (2018). Automatic Graphics Program Generation using Attention-Based Hierarchical Decoder. *CoRR*, abs/1810.1.